Real-Time Nonintrusive Detection Drowsiness – Phase II

Final Report

Prepared by:

Xun Yu

Department of Mechanical and Industrial Engineering
University of Minnesota Duluth

Northland Advanced Transportation Systems Research Laboratory
University of Minnesota Duluth

CTS 10-16

Technical Report Documentation Page

1. Report No. CTS 10-16	2.	3. Recipients Accession No.	
4. Title and Subtitle Real-Time Nonintrusive Detection of Driver Drowsiness – Phase II		5. Report Date December 2010 6.	
7. Author(s) Xun Yu		8. Performing Organization Report No.	
9. Performing Organization Name and Address Department of Mechanical and Industrial Engineering University of Minnesota Duluth 1305 Ordean Court Duluth, MN 55812		10. Project/Task/Work Unit No. CTS Project #2009005 11. Contract (C) or Grant (G) No.	
12. Sponsoring Organization Name and Address Intelligent Transportation Systems Institute Center for Transportation Studies 200 Transportation & Safety Building 511 Washington Ave SE Minneapolis, MN 55455		13. Type of Report and Period Covered Final Report 14. Sponsoring Agency Code	
15. Supplementary Notes http://www.cts.umn.edu/Publications/ResearchReports/			

16. Abstract (Limit: 200 words)

This project is the extension of the Northland Advanced Transportation System Research Laboratory (NATSRL) FY 2008 project titled "Real-time Nonintrusive Detection of Driver Drowsiness," which aims to develop a real-time, nonintrusive driver drowsiness detection system to reduce drowsiness-caused accidents. Biosensor is built on the vehicle steering wheel to measure driver's heartbeat signals. Heart rate variability (HRV), a physiological signal that has established links to waking/sleepiness stages, thus can be analyzed from the pulse signals for the detection of driver drowsiness. The novel design of measuring heartbeat signals from biosensors on the steering wheel and seatback makes this drowsiness detection system one with almost no annoyance to the driver, and the use of this physiological signal can ensure the accuracy of drowsiness detection. In Phase I, a biosensor with a pair of electrodes built on steering wheel was tested for the measurement of heartbeat for HRV analysis. However, this design requires the driver put both hands on the steering wheel to measure the heart rate. In Phase II, a new biosensor is designed that can measure heart rate even when only one hand is on the steering wheel, which happens very often in real driving situations. More extensive lab tests were carried out to study the change of HRV signals with driver drowsiness.

17. Document Analysis/Descriptors Drowsiness, Heart rate, Physiological aspects, Sensors		18. Availability Statement	
19. Security Class (this report) Unclassified	20. Security Class (this page) Unclassified	21. No. of Pages 37	22. Price

Real-Time Nonintrusive Detection of Driver Drowsiness

Final Report

Prepared by:

Xun Yu

Department of Mechanical and Industrial Engineering
University of Minnesota Duluth

Northland Advanced Transportation Systems Research Laboratory
University of Minnesota Duluth

December 2010

Published by:
Center for Transportation Studies
University of Minnesota
200 Transportation and Safety Building
511 Washington Ave. S.E
Minneapolis, MN 55455

Acknowledgements

The authors wish to acknowledge those who made this research possible. The study was funded by the Intelligent Transportation Systems (ITS) Institute and Northland Advanced Transportation System Research Laboratory (NATSRL). ITS is a program of the University of Minnesota's Center for Transportation Studies (CTS). Financial support was provided by the United States Department of Transportation's Research and Innovative Technologies Administration (RITA). NATSRL is a transportation research program at the University of Minnesota Duluth and its partners include the Minnesota Department of Transportation, the ITS Institute, St. Louis County and the City of Duluth.

We thank Dr. Eil Kwon, director of NATSRL, for many productive discussions.

We also thank the hard work of the students involved in this project: master degree graduate students Ms. Shan Hu and Mr. Ye Gu, and undergraduate student Mr. Ryan Bowlds.

Table of Contents

List of Figures

List of Tables

Executive Summary

This project is the extension of a Northland Advanced Transportation System Research Laboratory (NATSRL) FY 2008 project titled “Real-time Nonintrusive Detection of Driver Drowsiness”. In this FY09 Phase II project, a nonintrusive driver drowsiness detection system is developed by measuring and analyzing the driver’s heartbeat signals (ECG signal).

A piezoelectric polyvinylidene fluoride (PVDF) pulse wave sensor had been developed to measure the heart pulse from a driver’s palms for the purpose of detecting the driver’s drowsiness. The sensor is nonintrusive and can be easily installed on vehicle steering wheel. Once pulse wave signals are obtained, a driver’s instantaneous heart rate can be calculated from peak detection on pulse wave signals. To cancel the measurement noises induced by changing gripping force and vehicle vibration, an adaptive filter algorithm was used. To provide adaptive filter with noise reference inputs, which correlate with the noises present in pulse wave signals, the configuration of the sensor was specially designed. With the configuration, pulse wave signals with noise and two noise reference inputs to the adaptive filter were measured by the sensor system: one noise reference input is the “pure” changing gripping force from the bottom film; the other is acceleration of vibration in the direction perpendicular to the film surface. Experimental results showed that the sensor configuration working with the adaptive filter algorithm can provide clear pulse wave signals for heart pulse peak detection, even with the presence of gripping force noise and vehicle vibration noise

A two-hour driving simulation was conducted on seven human subjects in a driving simulator. Heart rate variability (HRV) analysis on the two-hour heart rate time series showed that low-frequency/high-frequency (LF/HF) ratio had a decreasing trend as all subjects became drowsy, although the slopes of trend were different among subjects. The driving simulation results show that the proposed sensors were successful in continuously monitoring driver’s heart rate and that the LF/HF ratio of HRV in frequency domain is promising to be used as an indicator for driver’s drowsiness detection.

Chapter 1 Introduction

1.1 Review of Driver Drowsiness Detection

Driver drowsiness is one of the major causes of serious traffic accidents. According to the National Highway Traffic Safety Administration (NHTSA) [1], there are about 56,000 crashes caused by drowsy drivers every year in US, which results in about 1,550 fatalities and 40,000 nonfatal injuries annually. The actual tolls may be considerably higher than these statistics, since larger numbers of driver inattention accidents caused by drowsiness are not included in above numbers [1]. The National Sleep Foundation also reported that 60% of adult drivers have driven while felling drowsy in the past year, and 37% have ever actually fallen asleep at the wheel [2]. For this reason, a technique that can real-time detect the drivers' drowsiness is of utmost importance to prevent drowsiness-caused accidents. If drowsiness status can be accurately detected, incidents can be prevented by countermeasures, such as the arousing of driver and deactivation of cruse control.

Sleep cycle is divided into nonrapid-eye-movement (NREM) sleep and rapid-eye-movement (REM) sleep, and the NREM sleep is further divided into stages 1-4. Drowsiness is stage 1 of NREM sleep – the first stage of sleep [3]. A number of efforts have been reported in the literature on the developing of drowsiness detection systems for drivers. NHTSA also supported several research projects on the driver drowsiness detection. These drowsiness detection methods can be categorized into two major approaches:

- **Imaging processing techniques** [4-11]: this approach analyzes the images captured by cameras to detect physical changes of drivers, such as eyelid movement, eye gaze, yawn, and head nodding. For example, the PERCLOS system developed by W. W. Wierwile *et. al.* used camera and imaging processing techniques to measure the percentage of eyelid closure over the pupil over time [8-10]. The three-in-one vehicle operator sensor developed by Northrop Grumman Co. also used the similar techniques [11]. Although this vision based method is not intrusive and will not cause annoyance to drivers, the drowsiness detection is not so accurate, which is severely affected by the environmental backgrounds, driving conditions, and driver activities (such as turning around, talking, and picking up beverage). In addition, this approach requires the camera to focus on a relative small area (around the driver's eyes). It thus requires relative precise camera focus adjustment for every driver.
- **Physiological signal detection techniques** [12-14]: this approach is to measure the physiological changes of drivers from biosignals, such as the electroencephalogram (EEG), electrooculograph (EOG), and electrocardiogram (ECG or EKG). Since the sleep rhythm is strongly correlated with brain and heart activities, these physiological biosignals can give accurate drowsiness/sleepiness detection. However, all the researches up to date in this approach need electrode contacts on drivers' head, face, or chest. Wiring is another problem for this approach. The electrode contacts and wires will annoy the drivers, and are difficult to be implemented in real applications.

To overcome the limitations of current drowsiness detection methods, this proposed research aims to develop a real-time, easy implementable, nonintrusive, and accurate drowsiness detection system. More specifically, we propose to embed biosensors into steering wheel to nonintrusively measure heartbeat pulse signals for the detection of driver drowsiness.

Time series of heartbeat pulse signal can be used to calculate the heart rate variability (HRV) – the variations of beat-to-beat intervals in the heart rate [15], and HRV has established differences between waking and sleep stages from previous psychophysiological studies [16-22]. The frequency domain spectral analysis of HRV shows that typical HRV in human has three main frequency bands: high frequency band (HF) that lies in 0.15 – 0.4 Hz, low frequency band (LF) in 0.04 – 0.15 Hz, and very low frequency (VLF) in 0.0033 – 0.04 Hz [15]. A number of psychophysiological researches have found that the LF to HF power spectral density ratio (LF/HF ratio) decreases when a person changes from waking into drowsiness/sleep stage [16-21], while the HF power increases associated with this status change [16, 22]. The HRV analysis therefore can be an effective method for the detection of driver drowsiness. Although a few studies have tried to use heart rate or HRV analysis to study driver fatigues [23-25] or driver stress level [26], no previous researches have tried to use HRV analysis for the driver drowsiness detection (driver fatigue is related but also different to driver drowsiness [1], e.g., a tired person not necessary feel sleepy and a sleepy person may not be tired). In this proposed research, heartbeat pulse signals will be measured by biosensors embedded in steering wheel, HRV will then be analyzed to detect driver drowsiness. The key to the proposed drowsiness detection approach is to have an accurate and non-invasive heart rate signal measurement system.

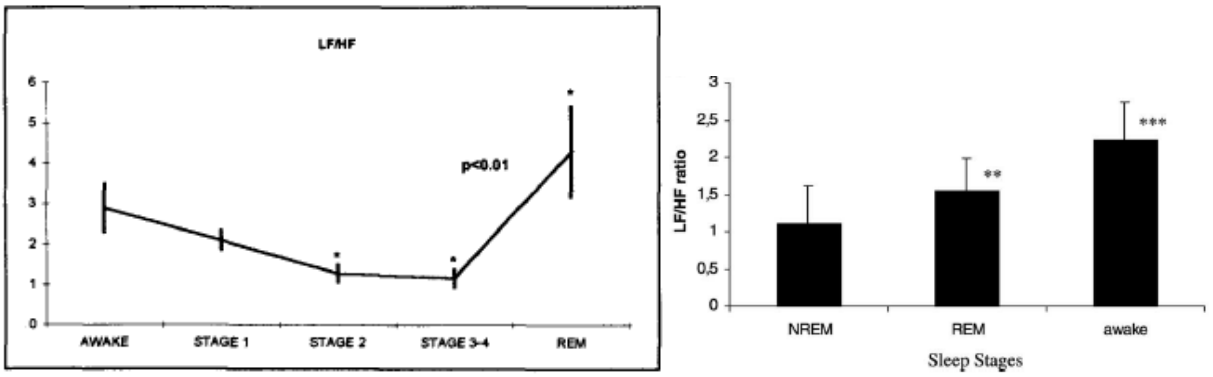

(A) (B)

Figure 1. Representative literature results showing the changes of LF/HF ratio in various sleep stages: (A) was cited from reference [19], (B) was cited from reference [20].

1.2 Review of Heart Rate Measurement Techniques

Comparing all the techniques available to detect drowsiness, heart-rate-based approach has the best potential: heart rate measurement doesn't require electrodes to be placed on special locations on human which makes it easy to adjust to different users; the relationship between HRV and sleep stages make it possible for heart-rate-based approach to predict driver's drowsiness and give out pre-warning; nonintrusive heart rate measurement is available in literature.

Since HRV is typically measured and analyzed from heart rate time series, sensors that can accurately measurement heart rate are utmost important to consider first. Typically, heart rate is obtained from ECG signals. Although ECG measurement techniques are well developed, most of them involve electrode contacts on chest or head, for example the conventional fixed-on-chest Ag-AgCl electrodes. Wiring and discomfort problems inherent in those techniques prevent their implementations on vehicles. Those heart rate monitor for fitness equipments also need a chest belt or needs both hands to touch a device to measure heart rate. Recently, several research groups have tried to develop non-contact ECG measurement using active electrodes [27-30]. Basically, electrodes with build-in amplifier circuit were placed on chair or bed (the electrodes thus are not directly contact with skin). The amplifier circuit also mediates the high impedance of cloths between the electrodes and skin. However, all of the non-contact ECG measurement is developed for use on office chairs or on a hospital bed. Measuring ECG in the office and hospital environment is different from measurement on vehicles. Given the vehicle's dynamical environment, unexpected measurement interference can come in. However, it is worth a try to reproduce such non-contact ECG measurement systems in this research to find out if those systems are effective in the environment setting of a vehicle. The other approach to obtain HRV signal is the detection of heart pulse wave on artery as the blood flow in artery reflects the cardiac rhythm [31-34]. Heart pulse wave is typically measured with finger-tip photoplethysmography (PPG) that use optical method to detect the blood flow rhythms, which is also an intrusive measurement with a clip-like device attached on finger tip. Rhee et al. developed a finger-ring type PPG sensor [33-35], which is less intrusive than normal PPG sensor but the little bulky ring is still annoy to drivers. Second, the ring type PPG sensor need precise position adjustment so that the blood flow will be in its optical transmit-receive path. Recently, the piezoelectric films have been utilized to detect heart pulse waves [36-37]. Different from above optical methods for blood flow rhythm detection, piezoelectric films detect the dynamic pulse forces that arise from the blood flow. Because of its high piezoelectric response and flexibility, piezo-polymer PVDF (polyvinylidene fluoride) films have been investigated for heart pulse wave measurements. Another advantage is that PVDF films could be attached any part of the human body that has close-to skin arterial vessels, such as chest wall, wrist, and palm. Lin et al. [36] tried to measure the heart pulse wave from palm for drivers using PVDF films. This is a nonintrusive approach for the heart pulse rate measurement and very promising results were reported for still human positions. However, their heart pulse wave measurement is severely affected by the gripping force and vibrations. Because the frequency of gripping force and vibrations overlap with the frequency of hear pulse rate, those measurement noise could not be effectively eliminated by typical filtering circuits. Therefore, a technique for the elimination of those motion artifacts poses a major challenge for the development of a nonintrusive heart pulse measurement system and the following HRV analysis for driver drowsiness detection.

1.3 Summary of Phase I Research Results (FY2008 NATSRL Project)

In Phase I of this research project, we developed two nonintrusive real-time ECG measurement methods for drivers: one on steering wheel and the other one on driver seatback. In both methods, electrically conductive fabric (ECF) is to be used as ECG electrodes. ECF is textile plated with conductive metal (for example, copper). Because of its flexibility and stretchability, ECF is deformable corresponding to the contour of the steering wheel and seatback, and it won't induce much discomfort to the drivers. Figure 2 shows our preliminary designs of two ECG measurement methods.

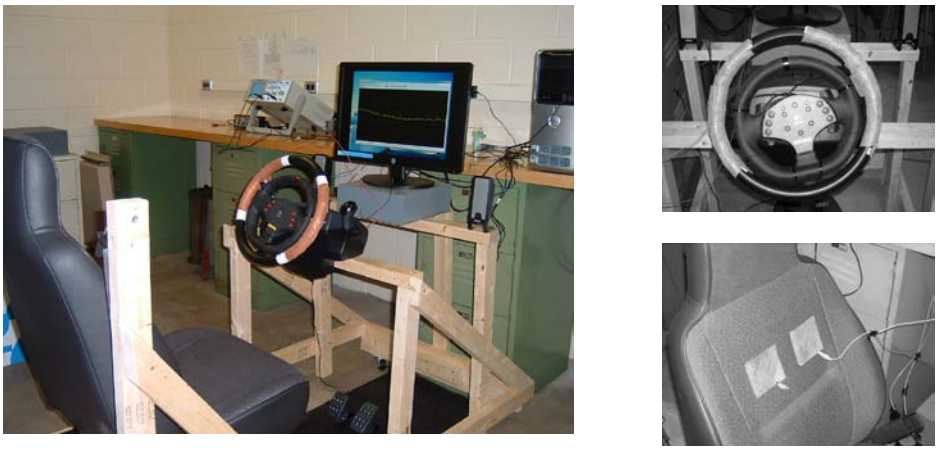

Figure 2. Preliminary design of ECG measurements – one on steering wheel, the other one on seatback.

In the first method (steering wheel), each half of steering wheel is wrapped with conductive fabric as electrode and is isolated to each other. Although electrode surface is directly contacted with driver's skin in this method, signals from electrodes on the steering wheel are still a little weak and noisy, and cannot be used for HRV analysis directly. To improve signal quality, signals from conductive fabric electrodes are to be filtered by a signal conditioning circuitry that consists of differential low pass, band pass and notch filters to amplify ECG signals and suppress noise (Figure 3). In the second method (driver seatback), two pieces of conductive fabric with the same dimension are placed on driver's seatback, so that the driver's heart is sandwiched between the two electrodes. Unlike electrodes in the first method, electrodes on the backrest are not contacted with drivers' skin directly. Thus, high impedance exists between electrode and skin due to the poor permittivity of commonly available clothes. To mediate the high impedance with low impedance required by the subsequent circuitry (the same signal conditioning circuitry used in the first method), an impedance matching circuit is proposed (shown in Figure 3), which is similar to a high pass filter with cut-off frequency $f = (2\pi RCs)^{-1}$ and a unit gain.

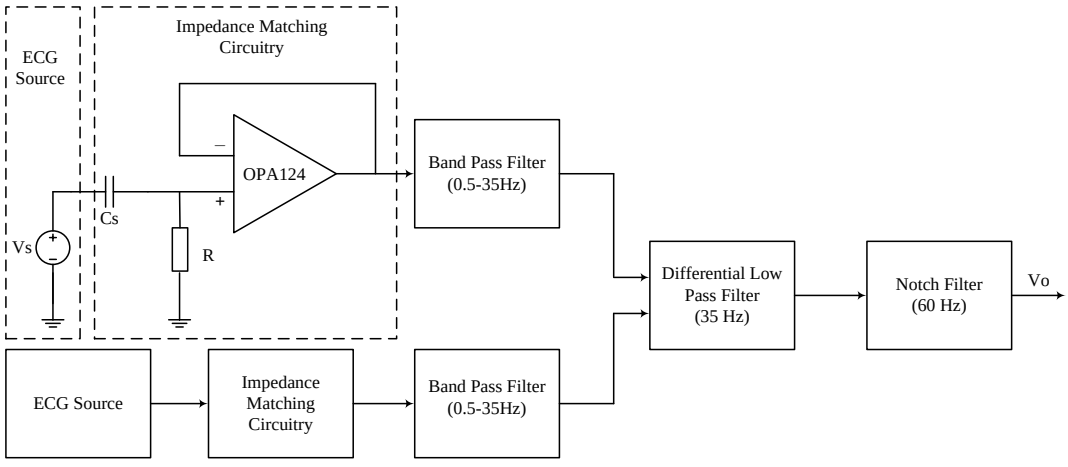

Figure 3. Diagram of the impedance matching circuit and signal conditioning circuit.

Figure 4 shows preliminary ECG measurement results from both methods, and Figure 5 shows the HRV LF/HF ratio of human subjects testing in driving simulator which shows a decreasing trend as the drive become tired and drowsy. As can been seen, clear ECG signals with satisfiable energy level could be obtained from both methods. However, there are several limitations of these ECG measurement techniques. For the method one, it requires driver puts both hands on the steering wheel to measure the ECG signal. However, drivers might use only one hand during the driving. For the second method (on seatback), the ECG signal is severely affected by the driver's body movement. Also, when the cloth is more than one thin layer, the impedance between electrode and skin becomes too large to be compensated by the circuit. Therefore, a new type nonintrusive heart rate sensor is needed to be developed, which is addressed in this Phase II research.

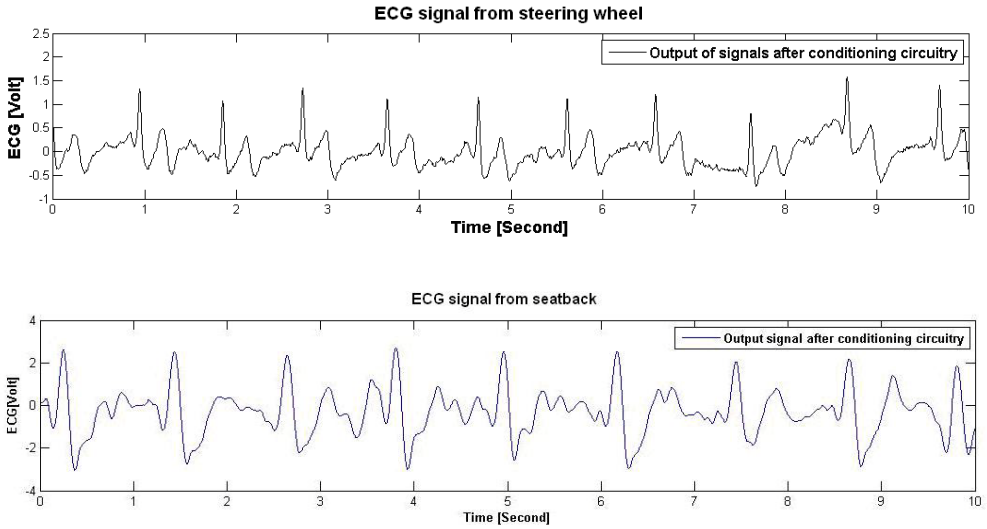

Figure 4. ECG signals collected from steering wheel and seatback.

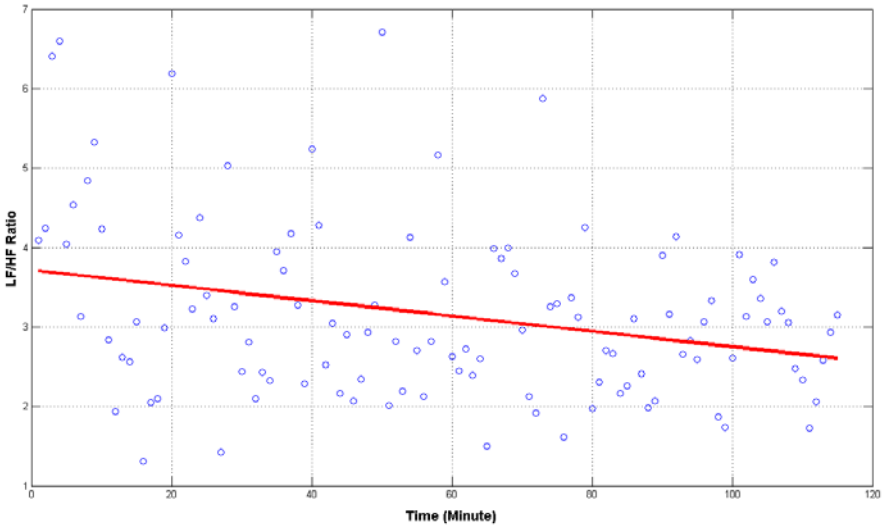

Figure 5. The LF/HF ratio during two-hour driving simulation for a human subject. The trend line is obtained by linear curve fitting.

Chapter 2 Nonintrusive Pulse Wave Sensor with Adaptive Noise Reduction for Vehicle Drivers

As discussed in Section 1.2, piezoelectric films have recently been utilized to detect heart pulse waves by detecting the dynamic pulse forces that arise from the blood flow. Because of its high piezoelectric response and flexibility, piezo-polymer PVDF (polyvinylidene fluoride) films have been investigated for heart pulse wave measurements. Lin et al. [36] tried to measure the heart pulse wave from palm for drivers using PVDF films. This is a nonintrusive approach for the heart pulse rate measurement and very promising results were reported for still human positions. However, their heart pulse wave measurement is severely affected by the gripping force and vibrations. Because the frequency of gripping force and vibrations overlap with the frequency of hear pulse rate, those measurement noise could not be effectively eliminated by typical filtering circuits. Therefore, a technique for the elimination of those motion artifacts poses a major challenge for the development of a nonintrusive heart pulse measurement system and the following HRV analysis for driver drowsiness detection.

In order to obtained accurate heart rate by peak detection in time domain, Lin *et al.* used a 0.4-1.8Hz band-pass filter to suppress noise [36]. This noise cancellation method does not work well with pulse wave peak detection. The band-pass filter flattens the heart pulse peaks and distorted the waveform of heart pulse, making it difficult to identify when exactly the peaks occur. In addition, the fixed-bandwidth filter cannot effectively eliminated noise introduced by changing gripping force and vibration, because the noise frequency range is not fixed and sometimes overlaps with the frequency of pulse wave (frequency range of normal resting heartbeat is1.00-1.67Hz). Other signal processing techniques such as Kalman Filter need a mathematic model of signal and the statistics of noise before it can detect signals from noisy background, thus is not appropriate for this application. On the other hand, adaptive filter is known for its ability to cancel noise without knowing the statistics of the noise beforehand. As a result, a feedforward adaptive filter approach is employed to eliminate the effects of changing gripping force and vehicle vibration on the heart pulse wave measurement in this research. To facilitate the adaptive filter in noise cancellation, a novel design of pulse wave sensor is also proposed.

2.1 Adaptive Filter Structure

Figure 6 illustrates the block diagram of the feedforward adaptive filter [38]. The primary input of the filter is the mix of desired pulse wave signal $s(n)$ and noises $n_1(n)$. The reference input $u(n)$ is the measurement of "pure" noise, which should be correlated with noise $n_1(n)$. If $y(n)$ is the output of the adaptive filter, the filter error is $e(n)= s(n)+ n_1(n)- y(n)$. Since the desired pulse wave signal $s(n)$ is uncorrelated with the noise $n_1(n)$, the mean-squared error (MSE) [39] of the adaptive filter is

$$\begin{aligned} E\left[e^2\right] &= E\left[\left(s_1+n_1\right)^2 - 2y\left(s_1+n_1\right)+y^2\right] \\ &= E\left[\left(n_1-y\right)^2 + s_1^2 + 2s_1n_1 - 2ys_1\right] = E\left[\left(n_1-y\right)^2\right] + E\left[s_1^2\right] \end{aligned} \tag{1}$$

Through minimizing MSE, filter error $e(n)$ will be the best estimation of the pulse wave signal. The MSE can be minimized if adaptive filter output $y(n)$ is a close estimation of $n_1(n)$. It is

obvious that if the reference input to adaptive filter *u(n)* is strongly correlated with $n_1(n)$, it is more likely the adaptive filter output $y(n)$ is close to $n_1(n)$. Least-mean-square (LMS) algorithm will be used to minimize the MSE by adapting the adaptive filter coefficient $w(n)$. Details and adaptation equations of LMS algorithm can be found in reference [39].

For adaptive filter, there are two important parameters: the filter order N and step size μ . The filter order N determines how many adaptive filter coefficients are used in the adaptive filter, i.e. the dimension of coefficient vector $w(n)$. Higher filter order gives more precise estimation of $n_1(n)$ at the adaptive filter output $y(n)$, but in the expense of computation power. Step size μ determines the convergence rate of the adaptive filter: higher value results in faster convergence. However, step size μ cannot be too large to cause instability. To guarantee the stability of adaptive filter step size μ must satisfies

$$0 < \mu < \frac{2}{NS_{\max}} \qquad (2)$$

where $S_{\max}$ is the maximum value of the power spectral density of reference input $u(n)$. In real application, filter order N and step size μ are empirically selected. In this research, the adaptive filter was empirically chosen to have a step size of 0.01 and an order of 16. With the chosen values, the adaptive filter achieved effective noise cancellation result with desired computational speed.

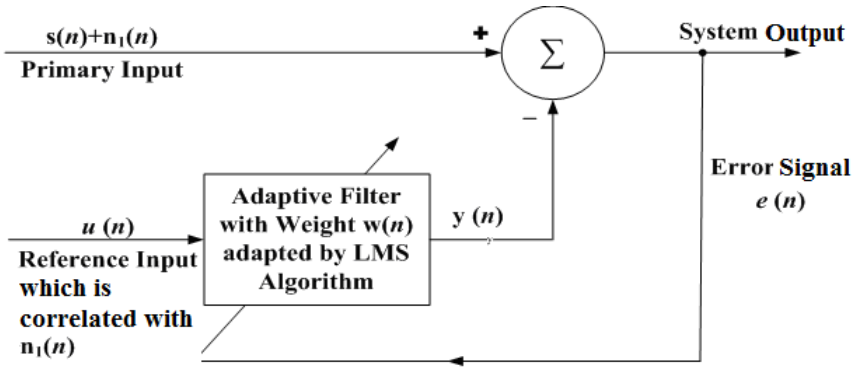

Figure 6. Block diagram of the feedforward adaptive filter.

During pulse wave measurement, there are two major sources of noise: the gripping force noise and vehicle vibration noise. In reality, these noise sources usually happened simultaneously. In addition, vehicle vibration can cause the relative movement between driver's hands and steering wheel, which in turn produces changing gripping force. The noise in raw pulse wave signals is likely from both noise sources. Therefore, a two-stage adaptive filter is employed in this work: one stage for the cancellation of gripping force noise and the second stage for the cancellation of vibration noise (details in Figure 7(a)).

2.2 Sensor Configuration Design for Adaptive Noise Cancellation

Based on the above discussion on adaptive filter algorithm, to extract pulse wave signals, or eliminate noise, it is important to provide a reference input $u(n)$ to the adaptive filter, which is strongly correlated with the noise presented in pulse wave signals. The configuration of the pulse wave sensor is specially designed to measure pulse wave signals and provide noise reference signals for the subsequent adaptive filter noise cancellation. To provide reference input to cancel noise caused by changing gripping force, instead of using one piece of PVDF film (Measurement Specialties Inc, DT1-028K PVDF film, size: 16mm x 40 mm x 40 μm), each sensor unit has a pair of two PVDF films, plus an isolation foam inserted between the two films (as shown in Figure 7 (a)). The PVDF film on top that contacts with the driver's palm (top film) is used to measure the mix of heart pulse wave and noise; the one on the bottom that contacts with the steering wheel (bottom film) is used to measure the gripping force noise. The foam is inserted to isolate heart pulse from the bottom film so that the bottom film can only pick up the change of gripping force but no pulse wave signals, so as to provide a reference input only correlated with noise present in the pulse wave signals. The measurement from top film, which is the mix of pulse wave signals and noise, will be introduced into the adaptive filter as primary input. Bottom film, which is the measurement of gripping force noise, will be the reference input to the first stage of the adaptive filter. The output of the first stage of adaptive filter will provide pulse wave signals without gripping force noise.

To cancel noise caused by vehicle vibration, an accelerometer (Analog Devices, ADXL321EB, 20mm × 20mm) is placed on the posterior side of the steering wheel near each pulse wave sensor in a way that one axis of the accelerometer (defined as perpendicular axis) is perpendicular to the PVDF film surface (as shown in Figure 7(a)). Consider the fact that PVDF film is sensitive to the dynamic bending stress caused by vibration perpendicular to film surface while insensitive to the dynamic shear stress caused by vibration parallel to film surface, only the output from the perpendicular axis is introduced into the adaptive filter as noise reference input to cancel vehicle vibration noise. With measurement of vehicle acceleration on perpendicular axis as the noise reference input to its second stage, the adaptive filter gives a real-time estimation of vibration noise present in the primary input. By subtracting the estimated noise from primary input, pulse wave signals without vibration noise can be obtained at the filter system output. As shown in Figure 7(b), an array of pulse wave sensors will be installed around the outer circle of the steering wheel to measure heart pulse wave, which can ensure the detection even with single hand driving only.

The adaptive filter is implemented with MATLAB in a PC. A National Instruments (NI) 6221 data acquisition board is used for data communication between the sensor and the PC. The sampling frequency of the data acquisition is 200Hz, which is high enough for pulse wave measurement.

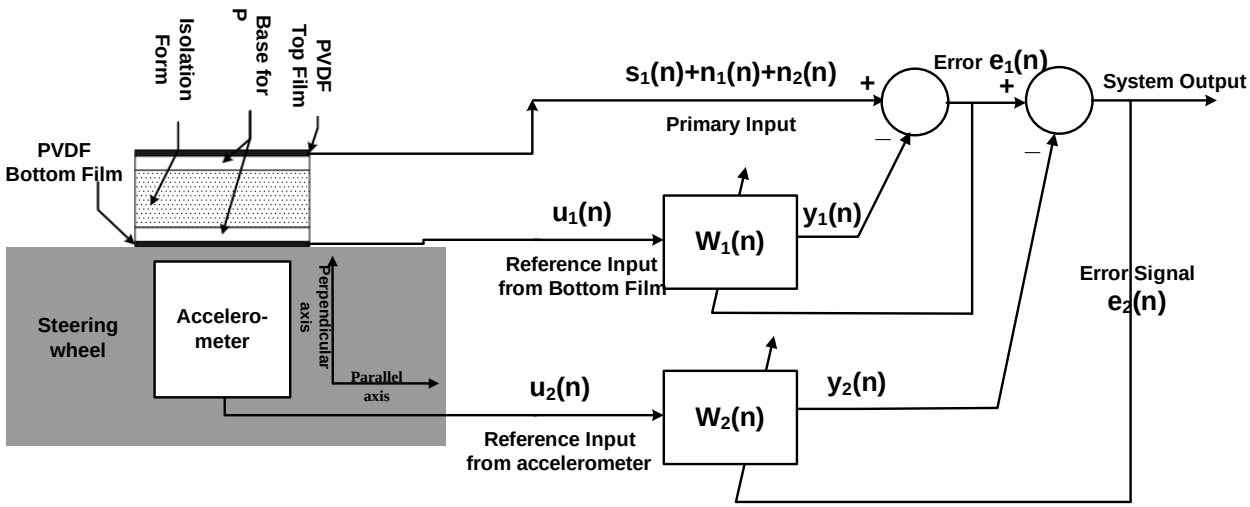

(a)

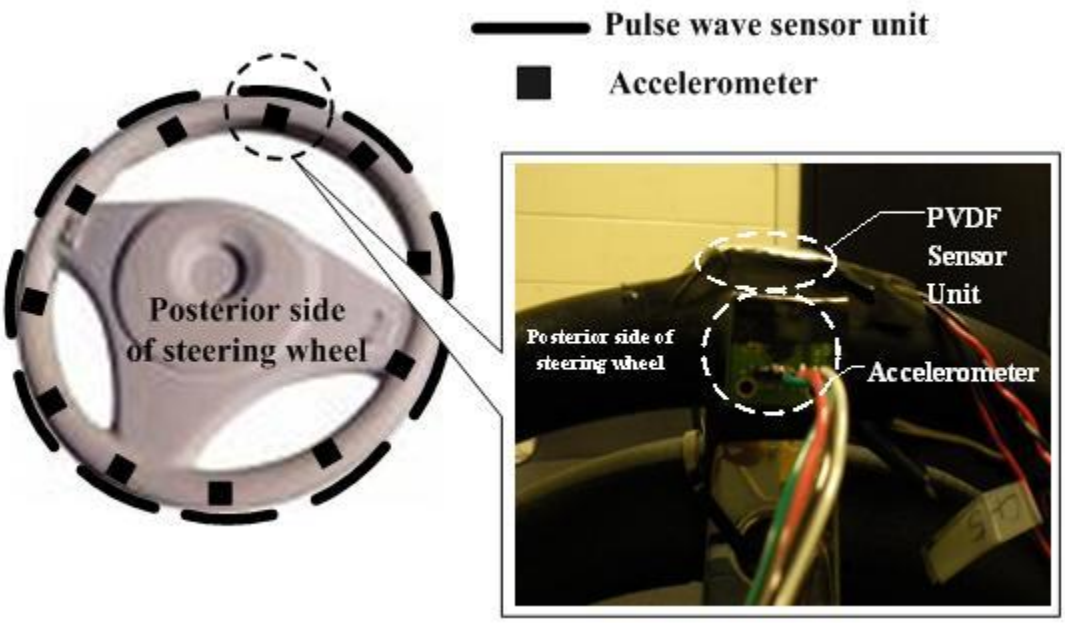

(b)

Figure 7. (a) Configuration design of the pulse wave sensor unit. (b) Layout of pulse wave sensor units and accelerometer on the steering wheel.

Chapter 3 Heart Pulse Wave Measurement Results

3.1 Heart Pulse Wave Measurement with Changing Gripping Force

To test the effectiveness of pulse wave measurement with the presence of gripping force noise, the subjects were asked to randomly change their gripping force during the measurement. Figure 8 shows the heart pulse wave measurement with changing gripping force. Figure 8(a) is the original signal measured by Top PVDF Film, which is clear for most still positions but is heavily polluted when there is gripping force changes (the gripping force is shown in Figure 8(c) as measured by Bottom PVDF Film). Figure 8(b) shows the pulse wave signal after the adaptive noise filter. With the noise cancellation, individual heart pulses are much easier to identify than original noisy pulse wave. The results show that the waveform of the pulse wave signals are well preserved by adaptive filter while the noise is removed. The result demonstrates that the configuration of pulse wave sensor is effective in measuring pulse wave signals and the Bottom PVDF Film can provide effective noise reference for the adaptive filter to eliminate gripping force noise.

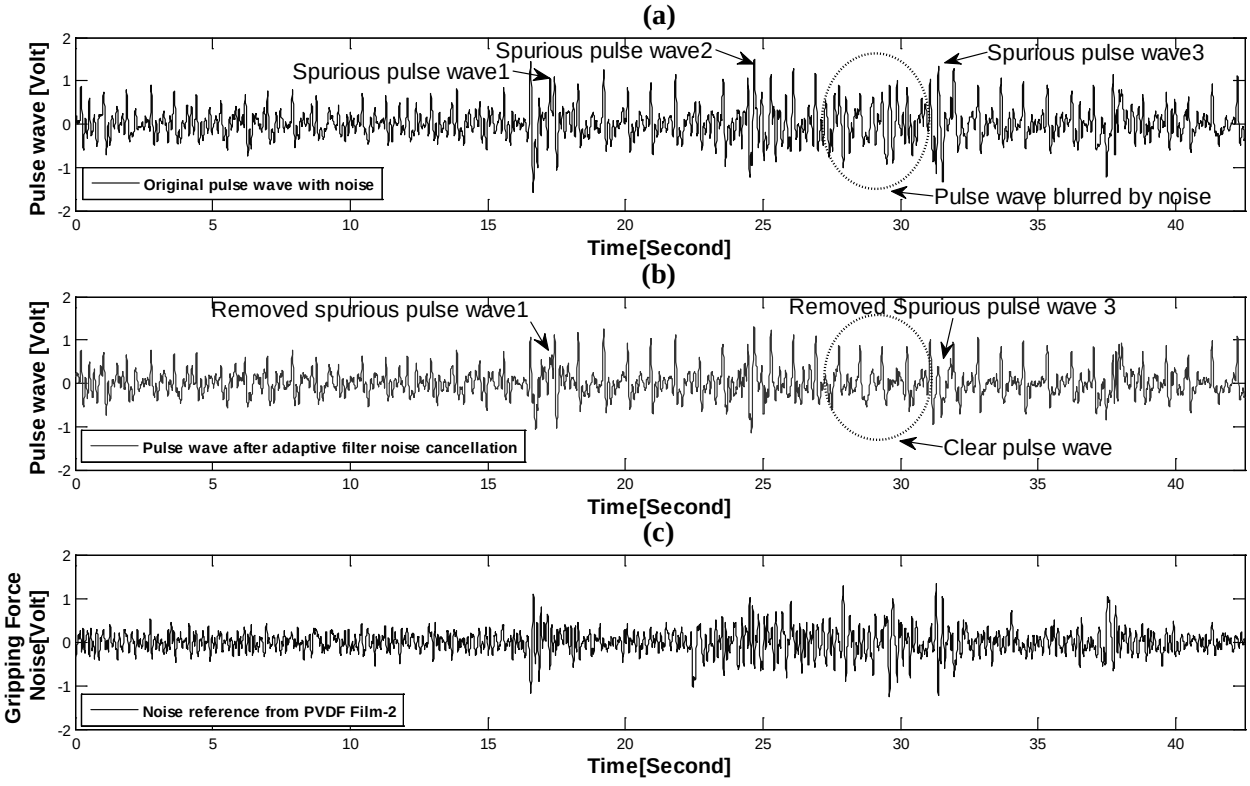

Figure 8. Noise cancellation result from adaptive filter. (a) is the pulse wave with noise from top PVDF film, (b) is the pulse wave after adaptive filter noise cancellation, (c) is the noise reference for adaptive filter from bottom PVDF film.

3.2 Heart Pulse Wave Measurement with Vehicle Vibration

To test the effectiveness of pulse wave measurement in the presence of vehicle vibration noise, the test rig was randomly vibrated by another person other than the subjects. In addition, the subjects were asked to control their gripping force at a constant level so as to eliminate changing gripping force. Figure 4 shows the pulse wave measurement result when random vibration was applied to the steering wheel. Figure 9 (a) is the original signal measured by Top PVDF Film: the vehicle vibration introduced high peaks around heart pulses, making the pulses difficult to identify. Figure 9 (c) shows the output of accelerometer, which is a voltage proportional to the steering wheel's acceleration in the direction perpendicular to the PVDF Film and is used as reference input for the adaptive filter. Figure 9 (b) shows the noise cancellation results from adaptive filter. The high peaks introduced by vibration were effectively eliminated, leaving the heart pulses easy to identify. The results demonstrate that the configuration of accelerometer can provide good noise reference for the adaptive filter to cancel vehicle vibration noise.

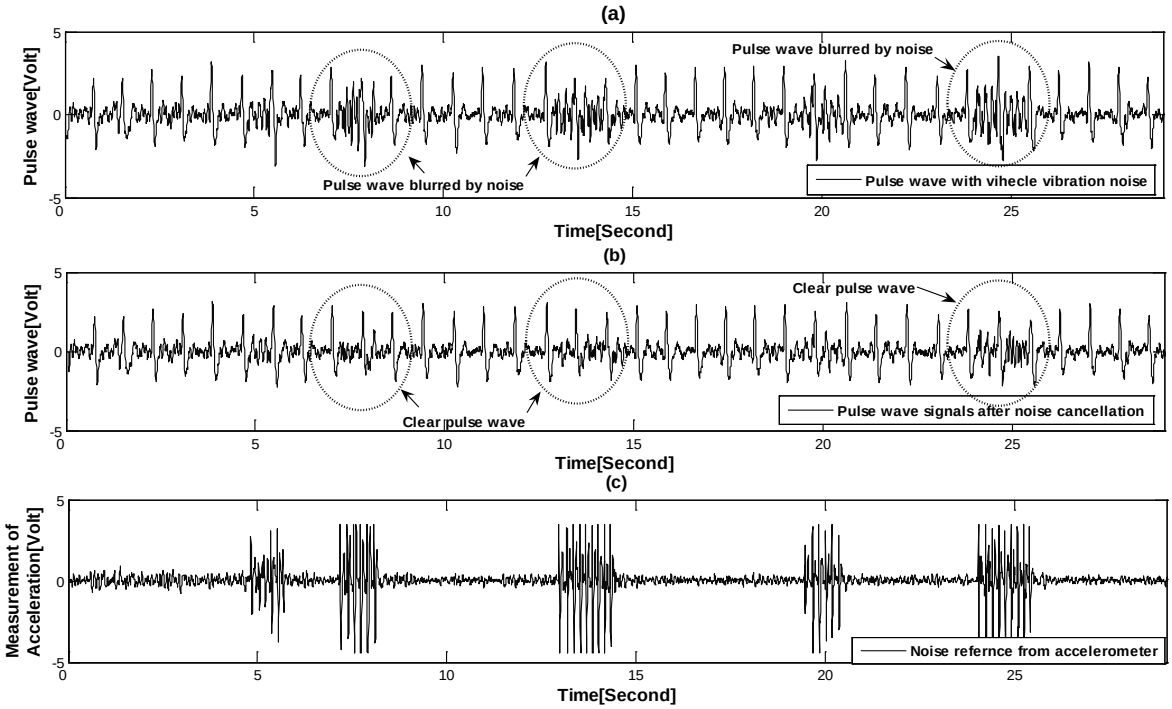

Figure 9. Noise cancellation result from adaptive filter with presence of vehicle vibration. (a) is the pulse wave with vehicle vibration noise, measured by top PVDF film, (b) is the pulse wave after adaptive filter, (c) is the measurement of acceleration in the direction that is perpendicular to the top PVDF film.

3.3 Heart Pulse Wave Measurement with Both Gripping Force Noise and Vehicle Vibration

To test the effectiveness of pulse wave measurement with the presence of gripping force noise and vehicle vibration, the test rig was vibrated by another person while the subjects were asked to randomly change gripping force. The two-stage adaptive filter with two reference inputs proposed in Figure 8 was used for noise cancellation. Figure 10 shows the measurement and

noise cancellation results. Figure 10(a) is the raw pulse wave signals measurement with both changing gripping force and vehicle vibration: pulse wave signals are blurred by noise and spurious pulse wave is introduced. In Figure 10(b), after adaptive filter noise cancellation, the blurred pulse wave signals are picked up from noisy background and spurious pulse wave is successfully suppressed. It demonstrates that the sensor configuration provides two effective noise reference inputs to the two-stage adaptive filter: acceleration of vibration perpendicular to PVDF film surface (Figure 10(c)) and changing gripping force (Figure 10(d)). With the two reference inputs, the proposed adaptive filter is capable of eliminating both gripping force noise and vehicle vibration noise simultaneously present in the pulse wave signals.

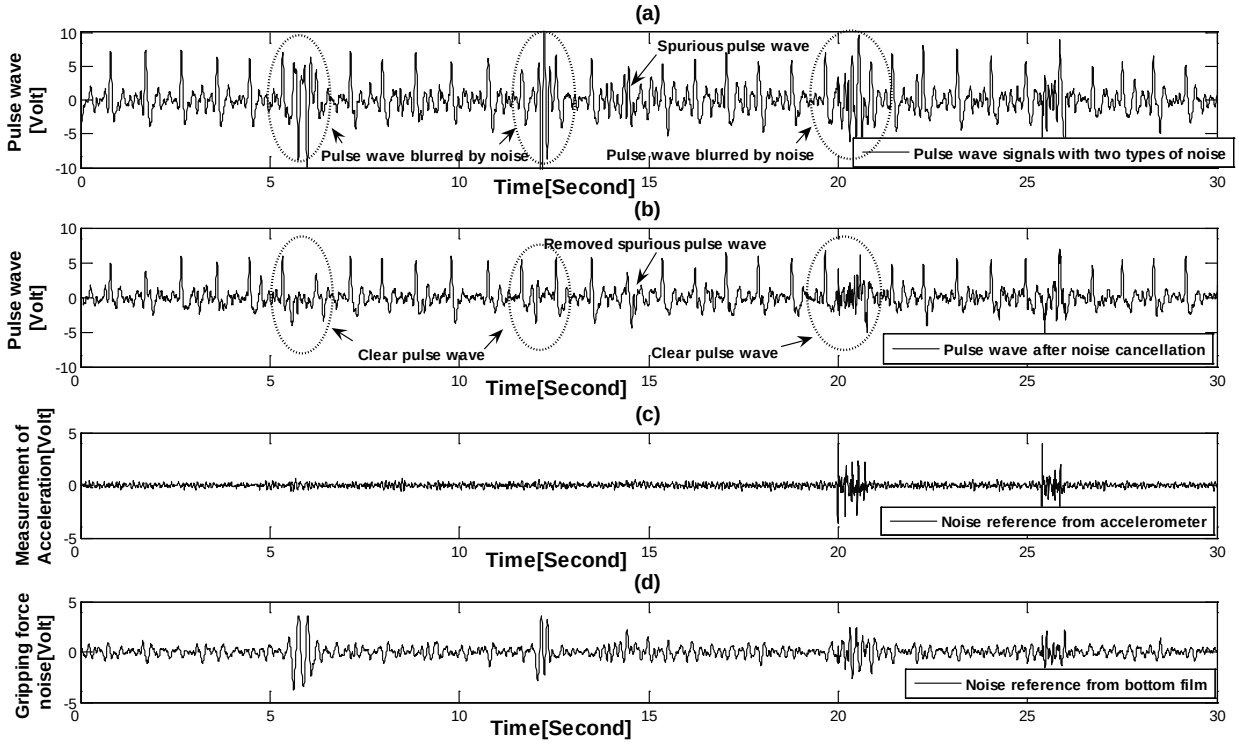

Figure 10. Noise cancellation results from adaptive filter with the presence of both gripping force noise and vehicle vibration noise. (a) Raw pulse wave signals with gripping force and vehicle vibration noise, (b) pulse wave signals after adaptive filter noise cancellation, (c) measurement of vehicle vibration acceleration perpendicular to film surface as one noise reference input for adaptive filter, (d) measurement of gripping force from bottom film as the other noise reference input or adaptive filter.

3.4 Computation of Heart Rate Time Series Using Pulse Wave Signal

To demonstrate that adaptive filter can improve peak detection accuracy, peak detection results on pulse wave signals with and without adaptive-filter noise cancellation (ANC) are compared. The pulse wave signal, which has 33 heart pulses in 30 seconds, is the one presented in Section 3.3. Figure 11 documents the comparison. Figure 11(a) is the peak detection results on pulse wave signals without ANC. Noise presented in the pulse wave deteriorate the accuracy of peak detection and cause 7 false heart pulses (marked as letter “F”) and 3 missing pulses (marked as dotted circle and letter “M”) in the result. Figure 11(b) is the peak detection results on pulse wave signals with ANC, which has less number of false heart pulses and missing pulses . The

performance with and without ANC are summarized and compared in Table 1. With ANC, the peak detection error rate decreased from 30.30% to 12.12%. Figure 6(c) is the heart rate time series computed based on the peak detection results shown in Figure 11(a) and (b). The upper and lower bound of normal resting heart rate (1-1.67Hz) are also marked in Figure 11(c). Heart rate time series without ANC fall out of the normal boundary more often than the time series with ANC, because more false and missing heartbeats happen during the peak detection.

(a)

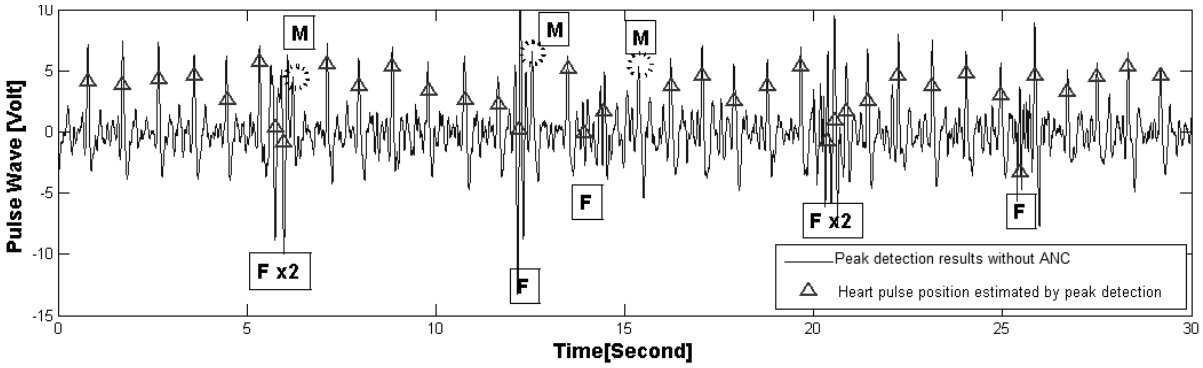

(b)

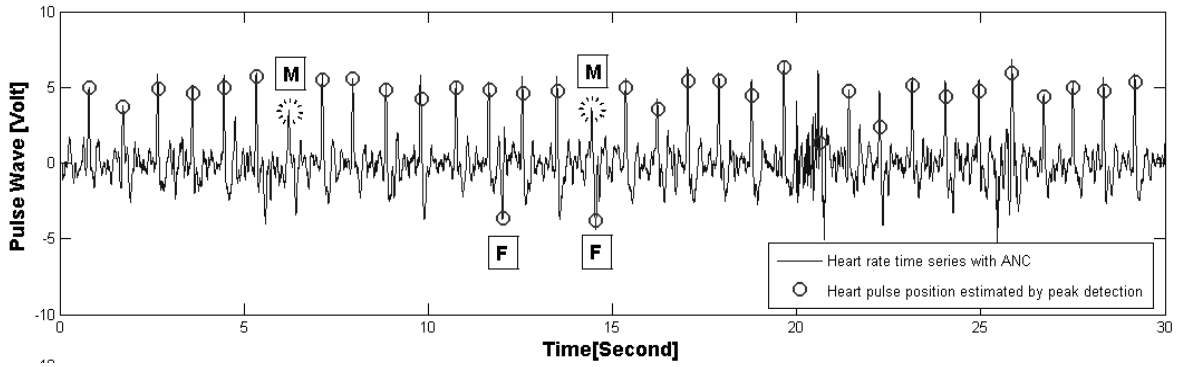

(c)

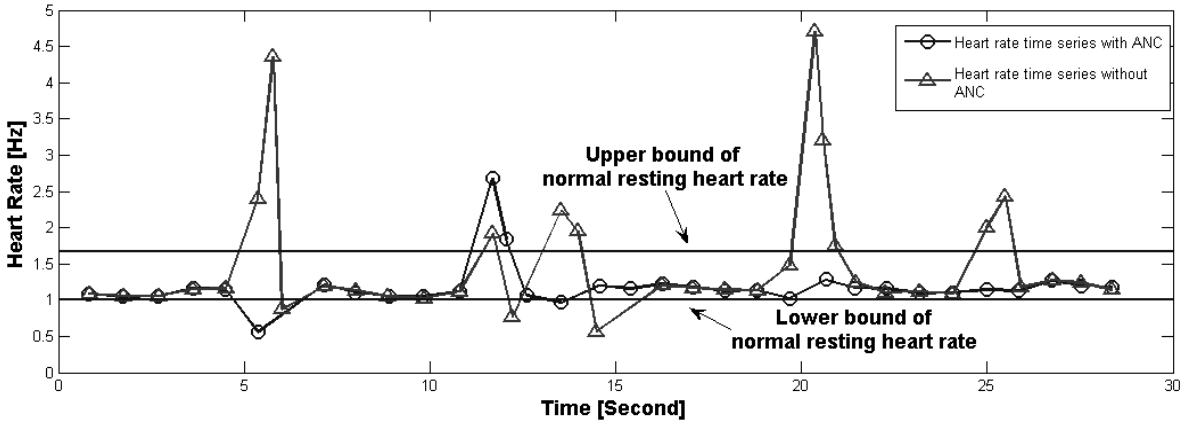

Figure 11. (a) Peak detection result on pulse wave signals without ANC, (b) Peak detection result on pulse wave signals with ANC, (c) Heart rate time series computed from peak detection results in (a) and (b).

Table 1. Performance of peak detection with and without ANC on pulse wave signals of 33 pulses

	Number of missing pulses	Number of false pulses	Total error rate (out of 33 pulses)
Peak detection with ANC	2	2	$\frac{2+2}{33} = 12.12\%$
Peak detection without ANC	3	7	$\frac{3+7}{33} = 30.30\%$

Chapter 4 HRV Analysis and System Tests

4.1 HRV Analysis for Drowsiness Detection

As clear heart pulse signals are obtained after noise cancellation procedure, HRV analysis will be performed to extract information for drowsiness detection. Figure 12 shows the flow diagram of the signal processing sequences.

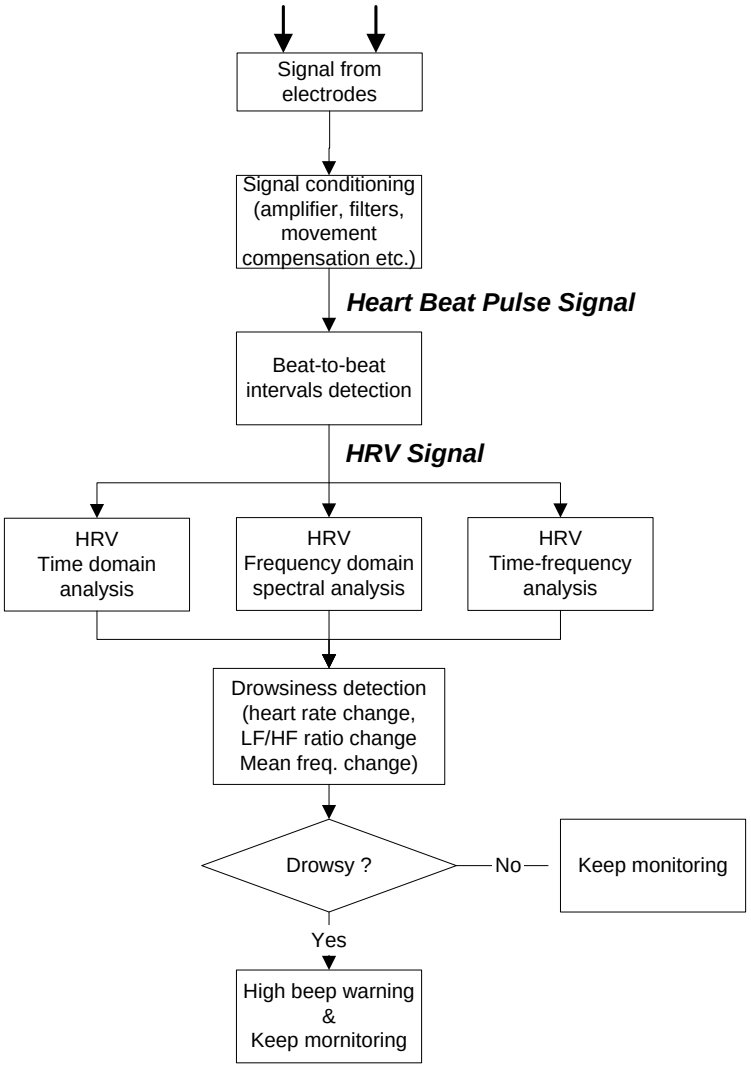

Figure 12. Flow diagram of the signal processing and HRV analysis system.

First, a peak detector computes the peak-to-peak interval (or heart rate) time series from ECG signals and pulse wave signals. Since the time intervals between peaks are not uniform, to enable the frequency analysis on heart rate time series, resampling is needed to turn the original heart rate time series into evenly sampled. Then the resampled time series is analyzed in two domains: frequency domain and time-frequency domain. In frequency domain, the power spectral density (PSD) of every two-minute heat rate time series will be estimated by the autoregressive method

[29]. Then the PSD is divided into three main frequency bands: high frequency band (HF) that lies in 0.15-0.4 Hz, low frequency band (LF) in 0.04-0.15 Hz, and very low frequency (VLF) in 0.0033-0.04 Hz. A number of psychophysiological researches found that the LF to HF ratio (LF/HF ratio) decreases when a person becomes sleepy [19, 20]. As a result, we choose to calculate LF/HF ratio as an indication of drowsiness instead of other kinds of HRV.

4.2 System Test Experimental Setup

A driving simulator as shown in Figure 13 is used to test the drowsiness detection system. The simulator has a screen to display the virtual reality driving environment, a real-size driver seat and a steering wheel. A subject was asked to drive with the simulator non-stop for two hours. The subject's heart rate was continuously recorded the ECG sensors or pulse wave sensor installed on the steering wheel. A camera was used to capture the video of driver's behavior, such as yawning, long-time eye closure, etc. The video will serve as a reference for driver's drowsiness level.

Figure 13. Layout of driving simulator.

4.3 Results of HRV Analysis during Driving Simulation

Totally seven subjects performed the driving simulation, three males and four females, age 19-48, all without known heart diseases. At the beginning, the subjects were not sleepy at all: the eye movements were quick and the body movement was active. However at the end, the drivers seemed sleepy at different levels: some started fidgeting and exhausted deep respiration, some blinked their eyes slowly and shut their eyelids sometimes. The females aged 48 and 21 and male aged 24 reported feeling drowsiness during the test.

Throughout the driving simulation, subjects' heart rate signals were recorded and HRV analysis was performed on the heart rate signals. Figure 14 shows example of the peak detection results of the pulse wave signals and the resulting peak-to-peak intervals. Though the detector missed a few peaks in pulse wave, the HRV analysis won't be affected too much.

Figure 15 shows an example of PSD estimated by autoregressive method and the range of low frequency and high frequency band. Figure 16 (a) to (g) show the HRV analysis in the frequency domain by autoregressive method throughout two hours for all nine subjects. The results of HRV analysis during the simulation are in accordance with previous psycho-physiological studies on the relationship between sleep stages and HRV, which answer the question whether results obtained when subjects were at rest can be applied to the situation when subjects were performing any tasks that introduce mental load. As they became drowsy during driving, all subjects' LF/HF ratios show a decreasing trend. However, the slopes of the trend vary among all subjects, because of difference between each individual's heart rate pattern and their various levels of drowsiness during the test.

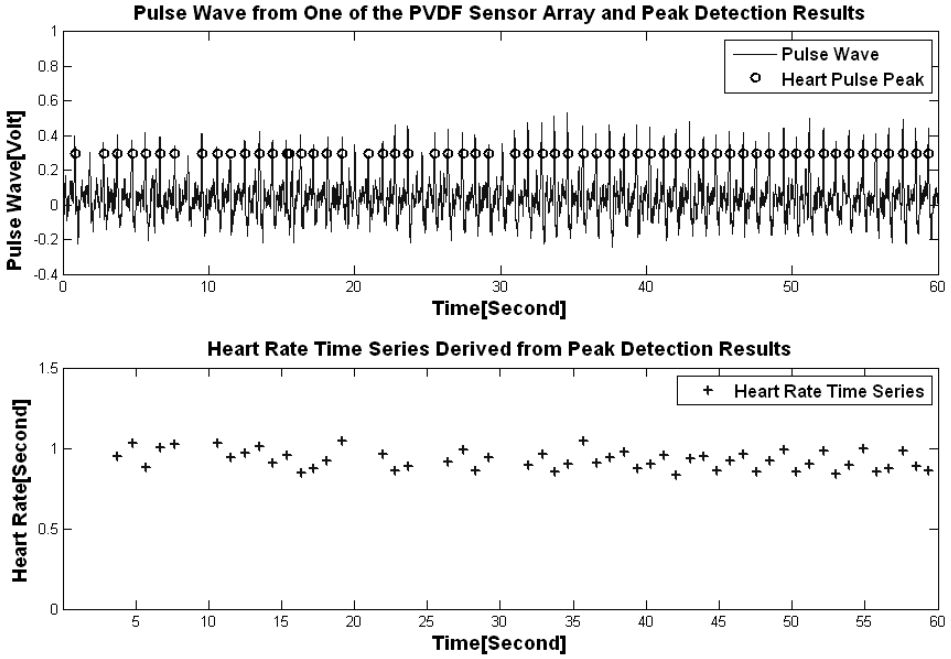

(b)

Figure 14. Peak detection results on the heart pulse wave signal.

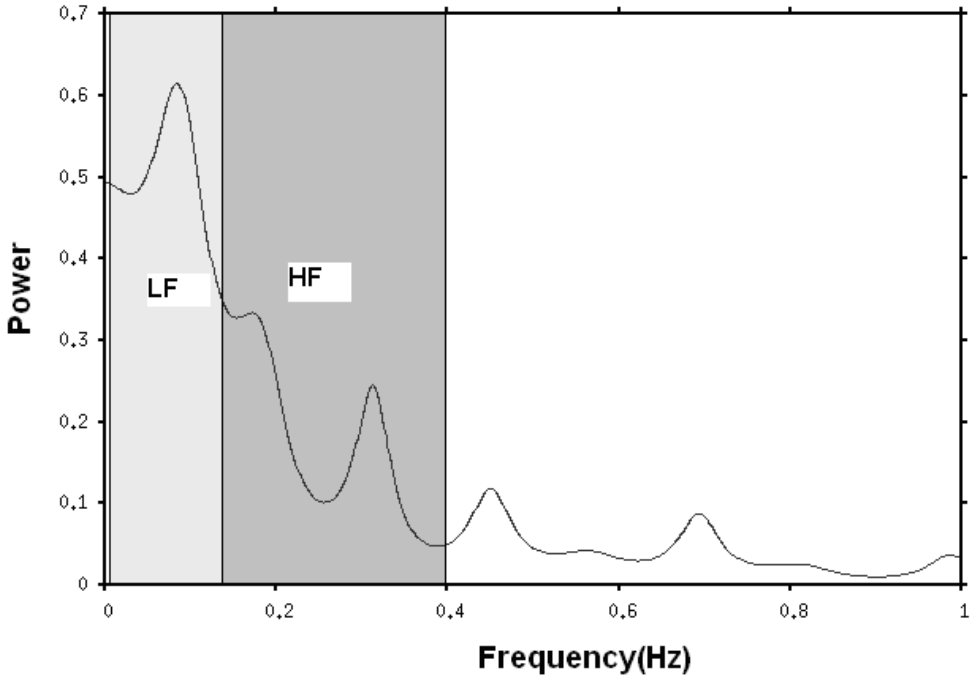

Figure 15. Example of heart rate spectrum estimated by autoregressive method and low frequency, high frequency range.

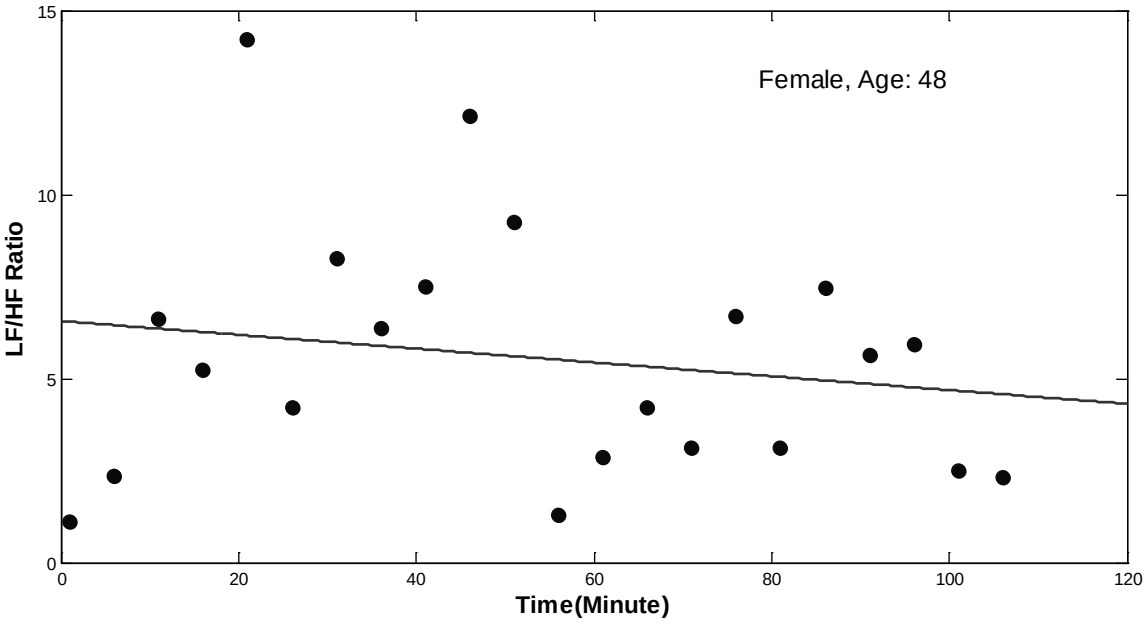

(a)

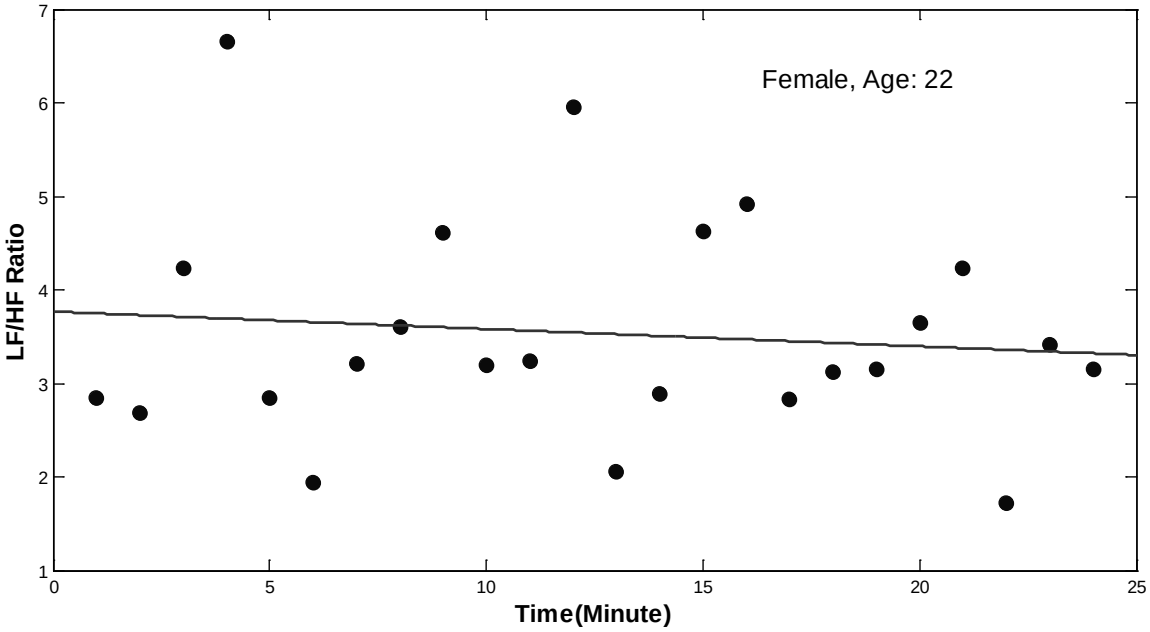
Female, Age: 22
LF/HF Ratio
Time(Minute)
1
2
3
4
5
6
7
0
5
10
15
20
25

(b)

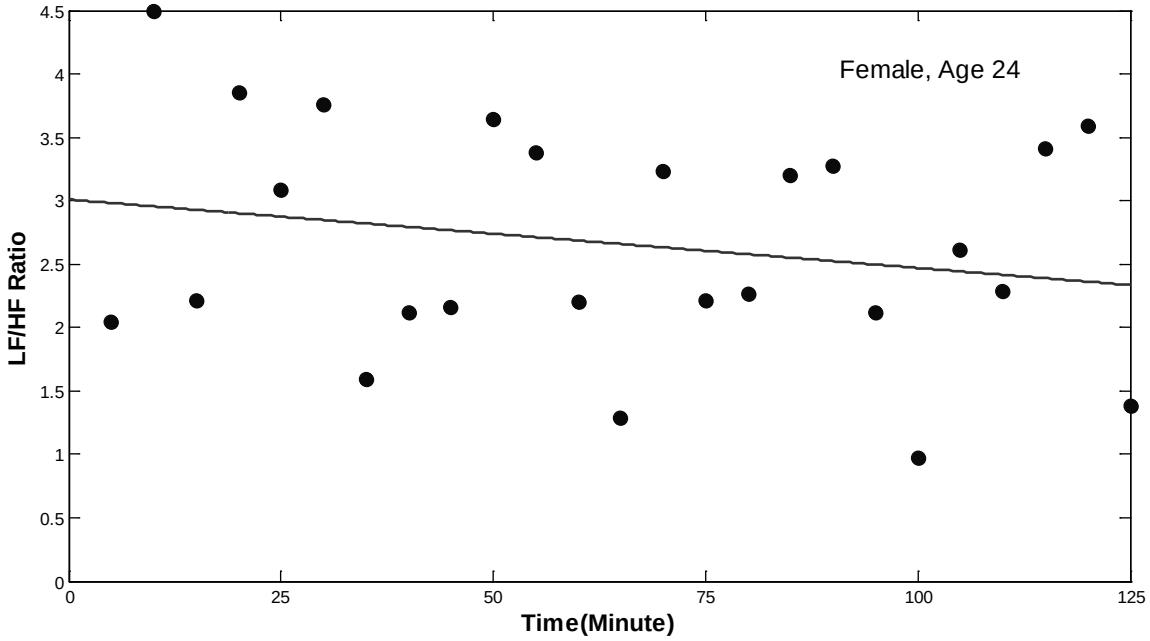
Female, Age 24
LF/HF Ratio
Time(Minute)
0
0.5
1
1.5
2
2.5
3
3.5
4
4.5
0
25
50
75
100
125

(c)

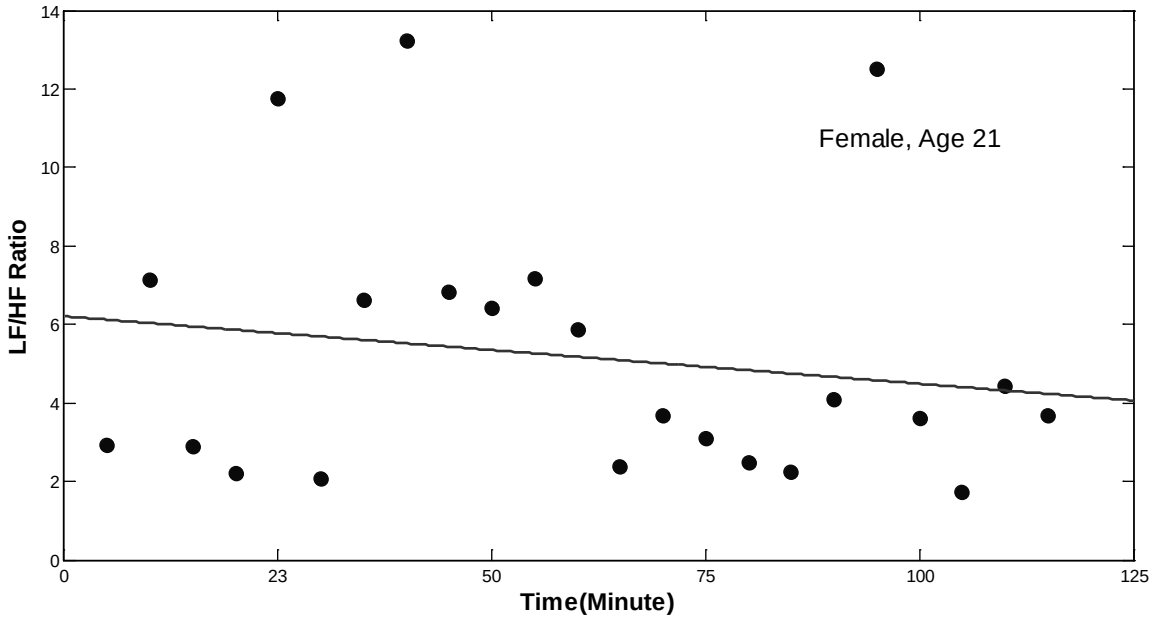
Female, Age 21
LF/HF Ratio
Time(Minute)
0
2
4
6
8
10
12
14
0
23
50
75
100
125

(d)

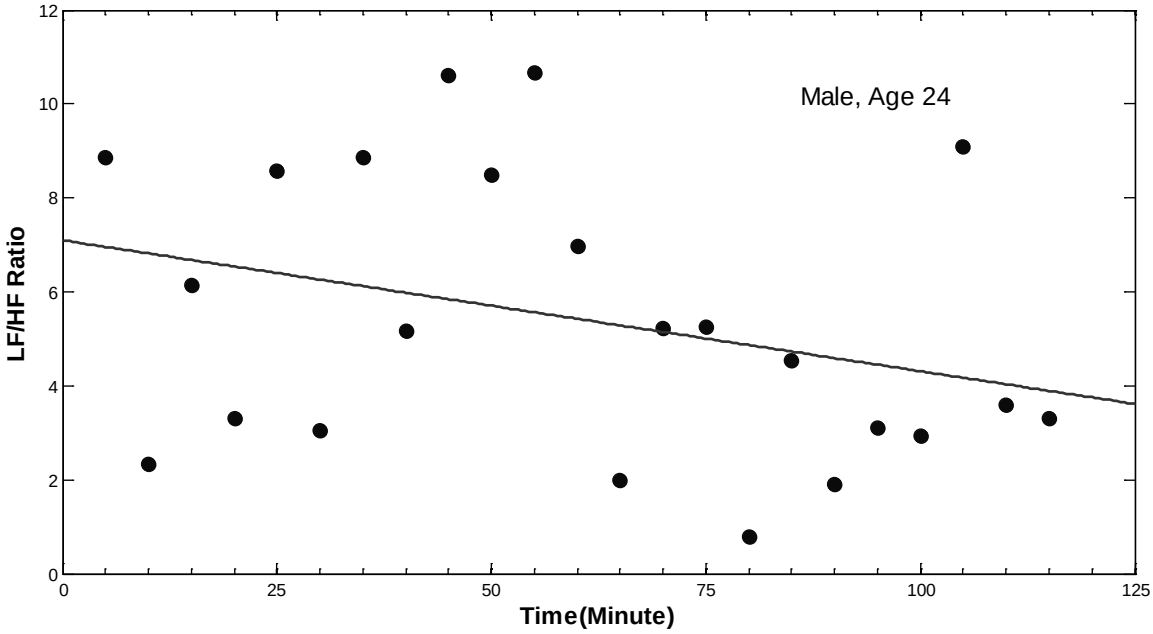
Male, Age 24
LF/HF Ratio
Time(Minute)
0
2
4
6
8
10
12
0
25
50
75
100
125

(e)

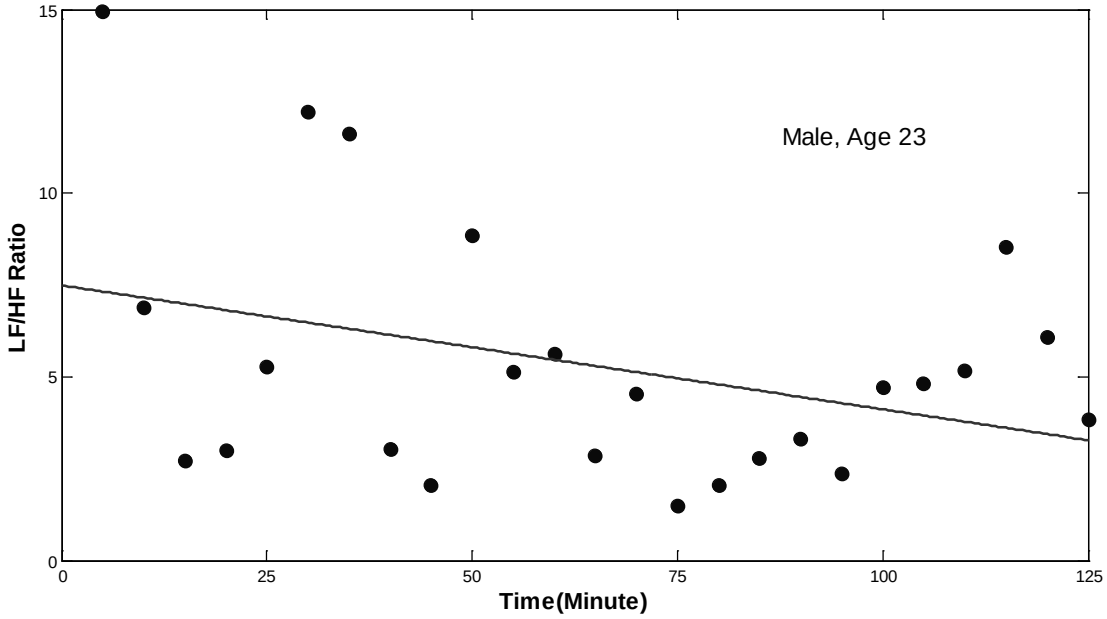

(f)

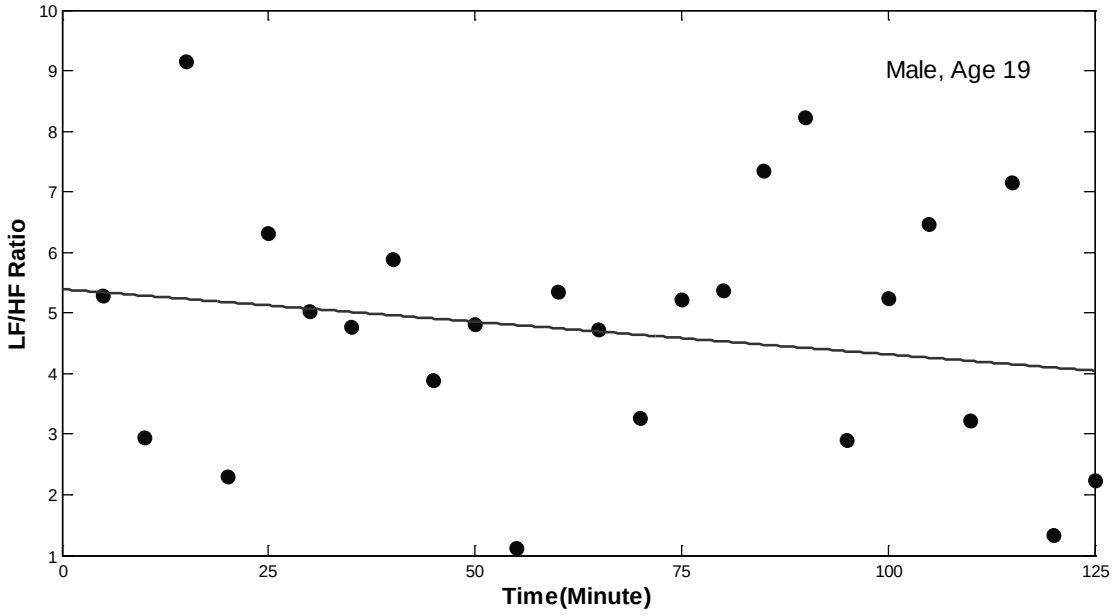

(g)

Figure 16. (a) to (g) LF/HF ratio through two hours of driving simulation taken by seven subjects, three males, four females, age 19-48.

Chapter 5 Conclusion and Discussion

In this research, PVDF pulse wave sensor had been developed to measure heart pulse from drivers' palms for the purpose of a driver's drowsiness detection. The sensor is nonintrusive and can be easily installed on vehicle steering wheel. Once pulse wave signals are obtained, a driver's instantaneous heart rate can be calculated from peak detection on pulse wave signals. To cancel the measurement noises induced by changing gripping force and vehicle vibration, an adaptive filter algorithm was used. To provide adaptive filter with noise reference inputs, which correlate with the noises present in pulse wave signals, the configuration of the sensor was specially designed. With the configuration, pulse wave signals with noise and two noise reference inputs to the adaptive filter were measured by the sensor system: one noise reference input is the "pure" changing gripping force from the bottom film; the other is acceleration of vibration in the direction perpendicular to the film surface. Experimental results showed that the sensor configuration working with the adaptive filter algorithm can provide clear pulse wave signals for heart pulse peak detection, even with the presence of gripping force noise and vehicle vibration noise

A two-hour driving simulation was conducted on seven human subjects in a driving simulator. HRV analysis on the two-hour heart rate time series showed that the LF/HF ratio had a decreasing trend as all subjects became drowsy, although the slopes of trend were different among subjects. The driving simulation results show that the proposed sensors were successful in continuously monitoring a driver's heart rate and that the LF/HF ratio of HRV in frequency domain is promising to be used as an indicator for a driver's drowsiness detection. Several limitations were also noticed during our research:

1. The pulse wave sensor measurement is still sensitive to hands' sling motions, which are different from the change of "pure" gripping force, and thus currently cannot be cancelled by the adaptive filter. Further improvement on the measurement system is needed.

2. Each individual has a unique HRV pattern (e.g., the different decreasing trend slopes observed from two subjects), thus future research is needed to create personalized drowsiness detection criterion.

3. The LF/HF alone had high variations in the time period studied; some other parameters that had a correlation with drowsiness should be included in the future drowsiness index.

References

[1] NCSDR/NHTSA Expert Panel on Driver Fatigue and Sleepiness, *Drowsy driving and automobile crashes*, National Highway Traffic Safety Administration (NHTSA) report, 1998.

[2] M. R. Rosekind, "Underestimating the societal costs of impaired alertness: safety, health and productivity risks," *Sleep Medicine*, vol. 6, pp. S21-S25, 2005.

[3] J. Gackenbach, *Sleep and dreams: A sourcebook*, New York : Garland, 1986.

[4] H. Ueno, M. Kaneda, and M. Tsukina, "Development of drowsiness detection system," *Proceedings of the 1994 Vehicle Navigation & Information Systems Conference*, Yokohama, Japan, Aug. 31-Sept. 2, pp. 15-20, 1994.

[5] P. S. Rau, "Drowsy driver detection and warning system for commercial vehicle drivers: field operational test design, data analysis, and progress," *National Highway Traffic Safety Administration*, paper number 05-0192, 2005.

[6] J. Chu, L. Jin, L. Guo, K. Guo, and R. Wang, "Driver's eye state detecting method design based on eye geometry feature," *2004 IEEE Intelligent Vehicles Symposium*, Parma, Italy, pp. 357-362, 2004.

[7] Q. Ji, Z. Zhu, and P. Lan, "Real-time nonintrusive monitoring and prediction of driver fatigue," *IEEE Transactions on Vehicular Technology*, vol. 53, pp. 1052-1069, 2004.

[8] W. W. Wierwille, S. S. Wreggit, C. L. Kirn, L. A. Ellsworth, and R. J. Fairbanks III, *Research on vehicle-based driver status/performance monitoring: development, validation, and refinement of algorithms for detection of driver drowsiness*, National Highway Traffic Safety Administration, U.S. DOT Tech Report No. DOT HS 808 247, 1994.

[9] W. W. Wierwille, M. G. Lewin, and R. J. Fairbanks III, *Final report: Research on vehicle-based driver status/performance monitoring, Part I, Part II, Part III*, National Highway Traffic Safety Administration, U.S. DOT Tech Report No. DOT HS 808 638, 1996.

[10] E. M. Ayoob, R. Grace, and A. Steinfeld, "A user-centered drowsy-driver detection and warning system," *Proceeding of the 2003 Conference on Designing for User Experiences*, San Francisco, CA, pp. 1-4, 2003.

[11] R. P. Hamlin, *Three-in-one vehicle operator sensor*, Transportation Research Board, National Research Council, IDEA program project final report ITS-18, 1995.

[12] H. J. Eoh, M. K. Chung, and S. H. Kim, "Electroencephalographic study of drowsiness in simulated driven with sleep deprivation," *International Journal of Industrial Ergonomics*, vol. 35, pp. 307-320, 2005.

[13] C. T. Lin, R. C. Wu, S. F. Liang, W. H. Chao, Y. J. Chen, and T. P. Jung, "EEG-based drowsiness estimation for safety driving using independent component analysis," *IEEE Transaction on Circuits and Systems*, vol. 52, pp. 2726-2738, 2005.

[14] S. K. L. Lal, A. Craig, P. Boord, L. Kirkup, and H. Nguyen, "Development of an algorithm for an EEG-based driver fatigue countermeasure," *Journal of Safety Research*, vol. 34, pp. 321-328, 2003.

[15] European Society of Cardiology and the North American Society of Pacing and Electrophysiology, "Heart rate variability: standards of measurement, physiological interpretation, and clinical use," *European Heart Journal*, vol. 19, pp. 354-381, 1996.

[16] S. Elsenbruch, M. Harnish, and W. C. Orr, "Heart rate variability during waking and sleep in healthy males and females," *Sleep*, vol. 22, pp. 1067-1071, 1999.

[17] L. Toscani, P. F. Gangemi, A. Parigi, R. Silipo, P. Ragghianti, E. Sirabella, M. Morelli, L. Bagnoli, R. Vergassola, and G. Zaccara, "Human heart rate variability and sleep stages," *The Italian Journal of Neurological Sciences*, vol. 17, pp. 437-439, 1996.

[18] M. H. Bonnet, and D. L. Arand, "Heart rate variability: sleep stage, time of night, and arousal influences," *Electroencephalography and Clinical Neurophysiology*, vol. 102, pp. 390-396, 1997.

[19] G. Calcagnini, G. Biancalana, F. Giubilei, S. Strano, and S. Cerutti, "Spectral analusis of heart rate variability signal during sleep stages," *Proceedings of the 16th Annual International Conference of the IEEE Engineering in Medicine and Biology Society*, Baltimore, MD, Nov. 3-6, vol. 2, pp.1252-1253, 1994.

[20] F. Jurysta, P. van de Borne, P. F. Migeotte, M. Dumont, J. P. Lanquart, J. P. Degaute, and P. Linkowski, "A study of the dynamic interactions between sleep EEG and heart rate variability in healthy young men," *Clinical Neurophysiology*, vol. 114, pp. 2146-2155, 2003.

[21] E. Vanoli, P. B. Adamson, B. Lin, G. D. Pinna, R. Lazzara, and W. C. Orr, "Heart rate variability during specific sleep stages - a comparison of healthy subjects with patients after myocardial infarction," *Circulation*, vol. 91, pp. 1918-1922, 1995.

[22] M. Tsunoda, T. Endo, S. Hashimoto, S. Honma, and K. I. Honma, "Effects of light and sleep stages on heart rate variability in humans," *Psychiatry and Clinical Neurosciences*, vol. 55, pp. 285-286, 2001.

[23] S. Milosevic, "Driver's fatigue studies," *Ergonomics*, vol. 40, pp. 381-389, 1997.

[24] N. Egelund, "Spectral analysis of heart rate variability as an indication of driver fatigue," *Ergonomics*, vol. 25, pp. 663-672, 1982.

[25] K, Jiao, Z. Y. Li, M. Cheng, and C. T. Wang, "Power spectral analysis of heart rate variability of driver fatigue," *Journal of Dong Hua University*, vol. 22, pp. 11-15, 2005.

[26] J. A. Healey, and R. W. Picard, "Detecting stress during real-world driving tasks using physiological sensors," *IEEE Transaction on Intelligent Transportation Systems*, vol. 6, pp. 156-166, 2005.

[27] M. Tsunoda, T. Endo, S. Hashimoto, S. Honma, and K. I. Honma, "Effects of light and sleep stages on heart rate variability in humans," *Psychiatry and Clinical Neurosciences*, vol. 55, pp. 285-286, 2001.

[28] C. J. Harland, T. D. Clark, and R. J. Prance, "Remote detection of human electroencephalograms using ultrahigh input impedance electric potential sensors" *Applied Physics Letters*, vol. 81, pp. 3284-3286, 2002.

[29] A. Aleksandrowicz, and S. Leonhardt, "Wireless and non-contact ECG measurement system - the "Aachen smart chair," *Acta Polytechnica*, vol. 47, pp. 68-71, 2007.

[30] Y. G. Lim, K. K. Kim, and K. S. Park, "ECG measurement on a chair without conductive contact" *IEEE Transactions on Biomedical Engineering*, vol. 53, pp. 956-959, 2006.

[31] T. Matsuda, and M. Makikawa, "ECG monitoring of a car driver using capacitively-coupled electrodes" *30th Annual International IEEE EMBS Conference*, Vancouver, British Columbia, Canada, August 20-24, pp. 1315-1318. 2008.

[32] M. Bolanos, H. Nazeran, and E. Haltiwanger, "Comparison of heart rate variability signal features derived from electrocardiography and photoplethysmography in healthy individuals," *28th IEEE EMBS Annual International Conference*, New York City, NY, Aug 30-Sept 3, pp. 4289-4294, 2006.

[33] N. Selvaraj, A. Jaryal, J. Santhosh, K.K. Deepak, and S. Anand, "Assessment of heart rate variability derived from finger-tip photoplethysmography as compared to electrocardiography," *Journal of Medical Engineering & Technology*, vol. 32, pp. 479-484, 2008.

[34] B. H. Yang and S. Rhee, "Development of the ring sensor for healthcare automation," *Robotics and Autonomous Systems*, vol. 30, pp. 273-281, 2000.

[35] H. H. Asada, P. Shaltis, A. Reisner, S. Rhee, and R. C. Huntchinson, "Mobile monitoring with wearable photoplethysmographic biosensors," *IEEE Engineering in Medicine and Biology Magazine*, May/June, pp. 28-40, 2003.

[36] Y. Lin, H. Leng, G. Yang, and H. Cai, "An intelligent noninvasive sensor for driver pulse wave measurement," *IEEE Sensors Journal*, vol. 7, pp. 790-799, 2007.

[37] S. Kärki and J. Lekkala, "Film-type transducer materials PVDF and EMFi in the measurement of heart and respiration rates," *30th Annual International IEEE EMBS Conference*, Vancouver, British Columbia, Canada, August 20-24, pp. 530-533, 2008.

[38] S. Haykin, *Adaptive Filter Theory*, third ed. Englewood Cliffs, NJ: Prentice-Hall, 1995.

[39] N. V. Thakor, and Y. S. Zhu, "Applications of adaptive filtering to ECG analysis: Noise cancellation and arrhythmia detection," *IEEE Transaction on Biomedical Engineering*, vol. 38, pp. 785-794, 1991.